

OPEN

Initial Staging of Locally Advanced Rectal Cancer and Regional Lymph Nodes

Comparison of Diffusion-Weighted MRI With ^{18}F -FDG-PET/CT

Milena Cerny, MD,* Vincent Dunet, MD,* John Olivier Prior, PhD, MD,† Dieter Hahnloser, MD,‡
Anna Dorothea Wagner, MD,§ Reto Antoine Meuli, MD,* and Sabine Schmidt, MD*

Purpose: The aim of the study was to compare diffusion-weighted MRI (DW-MRI) parameters with ^{18}F -FDG PET/CT in primary locally advanced rectal cancer (LARC).

Methods: From October 2012 to September 2014, 24 patients with histologically confirmed and untreated LARC (T3–T4) prospectively underwent a pelvic 1.5-T DW-MRI ($b = 0 \text{ s/mm}^2$, $b = 600 \text{ s/mm}^2$) and a whole-body ^{18}F -FDG PET/CT, before neoadjuvant therapy. The 2 examinations were performed on the same day. Two readers measured ^{18}F -FDG SUVmax and SUVmean of the rectal tumor and of the pathological regional lymph nodes on PET/CT and compared these with minimum and mean values of the ADC (ADCmin and ADCmean) on maps generated from DW-MRI. The diagnostic performance of ADC values in identifying pathological lymph nodes was also assessed.

Results: Regarding tumors ($n = 24$), we found a significant negative correlation between SUVmean and corresponding ADCmean values ($\rho = -0.61$, $P = 0.0017$) and between ADCmin and SUVmax ($\rho = -0.66$, $P = 0.0005$). Regarding the lymph nodes ($n = 63$), there was a significant negative correlation between ADCmean and SUVmean values ($\rho = -0.38$, $P = 0.0021$), but not between ADCmin and SUVmax values ($\rho = -0.11$, $P = 0.41$). Neither ADCmean nor ADCmin values helped distinguish pathological from benign lymph nodes (AUC of 0.24 [confidence interval, 0.10–0.38] and 0.41 [confidence interval, 0.22–0.60], respectively).

Conclusions: The correlations between ADCmean and SUVmean suggest an association between tumor cellularity and metabolic activity in untreated LARC and in regional lymph nodes. However, compared with ^{18}F -FDG PET/CT, ADC values are not reliable for identifying pathological lymph nodes.

Key Words: ^{18}F -FDG SUV, ADC, locally advanced rectal cancer, lymph nodes, MRI, PET/CT

(*Clin Nucl Med* 2016;41: 289–295)

Colorectal cancer is the second most common cancer, with 447,000 new cases per year in 2012, and the third most common cause of death from cancer in Europe. Rectal carcinoma represents 40% to 50% of colorectal cancers, among them 95% being adenocarcinoma.¹ Risk of local recurrence is substantial and correlates to

the extension and grade of the tumor and to the nodal status at initial presentation.²

Pelvic MRI and ^{18}F -FDG PET/CT are useful for staging and therapeutic management. Pelvic MRI allows for accurate definition of the distance to mesorectal fascia,^{3,4} which is a predictor of the local recurrence rate, as well as for definition of the regional nodal status. Although not commonly used in daily practice,⁵ ^{18}F -FDG PET/CT also helps in evaluating the nodal status and is especially performed for the detection of distant metastases.⁶ MRI and ^{18}F -FDG PET/CT are thus 2 complementary modalities for the initial staging of advanced rectal cancer. ^{18}F -FDG PET/CT provides the SUV, a quantitative measure of the metabolic activity of tumoral tissues that correlates with the tumor proliferative rate,⁷ whereas diffusion-weighted imaging (DWI) with ADC provides a quantitative measure of water diffusion in tissue that correlates with the tumor cell density and the histological differentiation grade.⁸ The relation between quantitative parameters of ^{18}F -FDG PET/CT and DWI has been assessed for various tumors and suggests a correlation between tumor metabolic activity and cellularity.^{9,10} However, only a few studies have assessed this relation in locally advanced rectal cancer (LARC).^{11,12}

The purposes of our study were to assess the relation between ADC and SUV for the primary tumor and the regional lymph nodes in LARC before neoadjuvant treatment and to assess the diagnostic performance of ADC values in identifying pathological lymph nodes.

MATERIALS AND METHODS

Population

From October 2012 to September 2014, 27 consecutive patients were prospectively enrolled in our study (19 men, 8 women; mean age, 63 ± 12 years [range, 45–87 years]). Inclusion criteria were a locally advanced, biopsy-proven rectal cancer (T3 and T4 stage) based on endorectal US (ERUS) and colonoscopic findings and no previous treatment of this tumor. Exclusion criteria were T1 and T2 stage rectal cancer revealed by imaging (ERUS and/or MRI), known contraindications to MRI, and incomplete baseline examinations. All patients underwent both baseline pelvic diffusion-weighted MRI (DW-MRI) and whole-body ^{18}F -FDG PET/CT on the same day for initial staging, before neoadjuvant treatment. Of 27 included patients, 3 patients were classified as T3 stage by ERUS, but downstaged to T2 stage after MRI. Because of the discrepancy between ERUS and MRI, these 3 patients were excluded. Twenty-four patients were thus included in the statistical analysis.

The institutional review board has approved the study, and written informed consent was obtained from all patients before inclusion in the study.

MRI Protocol

MRI examinations were performed on a 1.5-T scanner (Magnetom Aera; Siemens Healthcare, Erlangen Germany) using

Received for publication September 3, 2015; revision accepted January 5, 2016. From the Departments of *Diagnostic and Interventional Radiology; †Nuclear Medicine and Molecular Imaging; ‡Visceral Surgery, and §Oncology, Lausanne University Hospital, Lausanne, Switzerland.

M.C. and V.D. contributed equally to this work.

Conflicts of interest and sources of funding: none declared.

Correspondence to: Sabine Schmidt, MD, Department of Radiodiagnostic and Interventional Radiology, Lausanne University Hospital, Rue du Bugnon 46, 1011 Lausanne, Switzerland. E-mail: sabine.schmidt@chuv.ch.

Copyright © 2016 Wolters Kluwer Health, Inc. All rights reserved. This is an open-access article distributed under the terms of the Creative Commons Attribution-Non Commercial-No Derivatives License 4.0 (CCBY-NC-ND), where it is permissible to download and share the work provided it is properly cited. The work cannot be changed in any way or used commercially.

ISSN: 0363-9762/16/4104-0289

DOI: 10.1097/RLU.0000000000001172

a dedicated phase-array 18-canal body coil (Siemens Healthcare), with the patient in a supine position on the MR table. No rectal cleansing, rectal enema, or air insufflation was performed. After fasting for at least 6 hours before the MRI, all patients were intravenously injected with 20 mg of scopolamine butylbromide (Buscopan; Boehringer Ingelheim, Basel, Switzerland) or, if contraindicated, with 1 mg of glucagon (Glucagen; Novo Nordisk, Bagsvaerd, Denmark) to reduce artifacts due to bowel peristalsis. MRI protocol parameters were the same for all patients (Table 1). Three-plane (axial, sagittal, and coronal) T2-weighted turbo spin echo (TSE) images of the rectum were first obtained with an axial acquisition perpendicular to the rectal tumor. Axial T2-weighted TSE images of the upper pelvis including the iliac bifurcation were also acquired. Axial single-shot spin-echo echo-planar DWI sequences in 3 orthogonal directions (frequency encoding, phase encoding, and slice encoding) with 2 *b* values = 0 and 600 s/mm² were subsequently acquired from the iliac bifurcation to the anal verge. Pixel-to-pixel ADC maps were generated from DWI using Siemens software.

¹⁸F-FDG PET/CT Protocol

All PET/CT examinations were performed on a Discovery 690 PET/CT scanner (GE Healthcare, Milwaukee, Wis). After fasting for at least 6 hours before the examination, patients were intravenously injected with 248 ± 43 MBq (range, 160–374 MBq) of ¹⁸F-FDG. Blood glucose level was checked to be less than 8.3 mmol/L prior to administering ¹⁸F-FDG. A vertex-to-midhigh PET/CT acquisition (time-of-flight 3D mode; 7–9 steps of 2 minutes; mean duration, 16 ± 1 minutes; range, 14–18 minutes) was performed 66 ± 6 minutes (range, 55–76 minutes) after ¹⁸F-FDG administration. Step duration was not adjusted according to patient body mass index. It was preceded by an unenhanced MDCT (64-row detector, 120 kV, automatic tube intensity modulation, pitch 1.5, 0.5-second rotation time, 3.75-mm slice thickness) used for attenuation correction. PET data were reconstructed using an ordered-subset expectation maximization method with 8 subsets and 2 iterations.

PET/CT and MR Images Analysis

Two readers, one with 4 years of experience as a radiologist and the other with 8 years of experience as both a radiologist and a nuclear physician, blinded to ERUS and colonoscopic results, reviewed the MR and PET/CT examinations on a PACS workstation

(CARESTREAM PACS Client, version 11; Carestream Health, Rochester, NY) in consensus.

Rectal Cancer Analysis

For all tumors, the stage revealed by MRI (T3 or T4), the location within the rectum (lower, middle, or upper third), the distance to the anal verge in millimeters, the longitudinal extension of the tumor in millimeters, the presence (scored as follows: 0 if absent or 1 if present), and location (anterior, posterior, or lateral rectal walls) of spicules 3 mm or greater within the mesorectal fat were recorded.

The highest ¹⁸F-FDG SUV was automatically detected. Then, in consensus, the 2 readers drew ellipsoid ROIs of 1 cm² on the tumor area of the rectal wall containing the highest ¹⁸F-FDG SUV on axial PET images and measured the SUVmax and SUVmean of the rectal cancer (Fig. 1).

After spatial rigid coregistration of the DWI with the ¹⁸F-FDG PET/CT images, the same ROI was automatically transferred onto the ADC map generated from DWI. The ADCmin and ADCmean were then measured.

Regional Lymph Nodes Analysis

No pathological specimen was available in our untreated population, because all patients immediately underwent neoadjuvant radiochemotherapy after imaging. Therefore, for regional lymph node analysis, the combination of ¹⁸F-FDG PET/CT and morphological MRI criteria was considered as the standard of reference.¹³ Lymph nodes were defined as pathological when demonstrating a short axis of 6 mm or greater, round shape, loss of fatty hilum, indistinct borders, heterogeneous signal on T2-weighted MR images,⁵ and an ¹⁸F-FDG uptake higher than the background activity of soft tissues on PET/CT images. For comparison, the 2 readers also evaluated control lymph nodes that were defined as having a short axis of 6 mm or greater, oval shape, preserved fatty hilum, smooth borders, homogeneous signal on T2-weighted MR images, and an ¹⁸F-FDG uptake lower than the background activity of soft tissues on PET/CT-images. All the chosen control lymph nodes were located in the inguinal chain of patients who did not have any external iliac or inguinal pathological lymph nodes. For both pathological regional lymph nodes and control lymph nodes, ROIs (size range, 0.3–1 cm²) were drawn in consensus around the nodes, and SUVmax and SUVmean values were measured.

TABLE 1. Pulse Sequence Parameters

Parameters	Sagittal T2-Weighted TSE of the Rectum	Axial T2-Weighted TSE Perpendicular to the Rectal Tumor	Oblique Coronal T2-Weighted TSE of the Rectum	Axial T2-Weighted TSE of the Upper Pelvis	Diffusion Weight
Matrix size	384 × 384	320 × 320	320 × 320	320 × 320	160 × 160
Slice thickness, mm	4	3	3	3	5
Distance factor, %	20	20	20	20	10
Repetition time, ms	4000	6370	4000	4000	3200
Echo time, ms	103	99	99	103	55
Echo trains per slice (1)	8	11	11	11	
Flip angle, degrees	160	160	160	160	
Average	3	3	3	2	6
FoV, mm	180 × 289	180 × 289	180 × 289	220 × 354	350 × 563
Bandwidth, Hz/pixel	200	200	200	200	148
Acquisition time	3 min 22 s	3 min 38 s	4 min 34 s	3 min 6 s	1 min 34 s

(1) indicates means the number of echos per echo train and is a free variable (without units) in the international system; FoV, field of view.

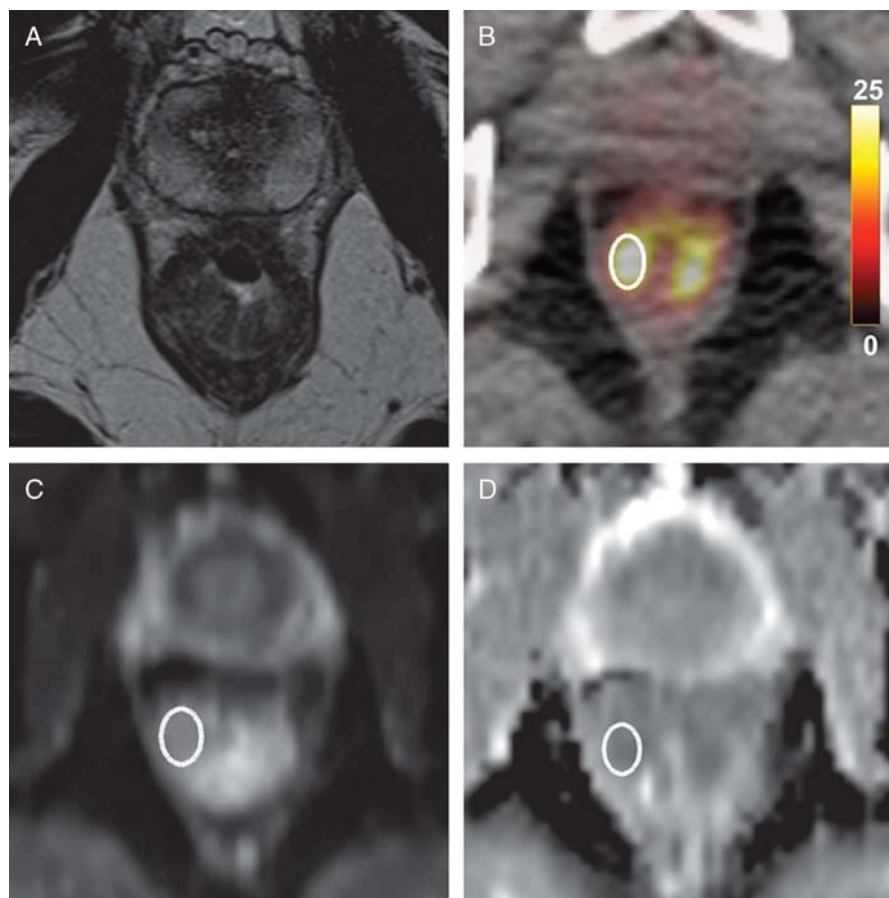


FIGURE 1. Locally advanced rectal cancer in a 50-year-old man. **A**, Axial T2-weighted MR image shows a T4-stage rectal tumor with predominant thickening of the right wall. **B**, Axial ^{18}F -FDG PET/CT demonstrates high tumor ^{18}F -FDG uptake (SUVmean = 10.5 g/mL, SUVmax = 14.7 g/mL). **C** and **D**, Axial diffusion-weighted image and ADC map show diffusion restriction within the tumor (ADCmean = $953 \times 10^{-6} \text{ mm}^2/\text{s}$, ADCmin = $882 \times 10^{-6} \text{ mm}^2/\text{s}$).

The ADCmin and ADCmean values of the lymph nodes were again measured by applying the same ROI on ADC maps after coregistration with ^{18}F -FDG PET/CT images (Fig. 2). The number, location, and size of all the pathological and control lymph nodes were also recorded.

Statistical Analysis

Data were analyzed using Stata 13.1 software (Stata Corporation, College Station, Tex). Continuous variables are presented as mean \pm SD, and categorical variables as number or percentage. The nonparametric Kruskal-Wallis test was used to compare SUVmax, SUVmean, ADCmin, and ADCmean between tumor subgroups. The same test was used to compare the size, SUVmax, SUVmean, ADCmin, and ADCmean of pathological versus control lymph nodes. We assessed the relations between SUVmax, SUVmean, ADCmin, and ADCmean of the rectal tumors and of the lymph nodes by computing the Spearman ρ correlation coefficient. Values of Spearman ρ values were interpreted as follows: 0 or less was poor, 0 to 0.20 was slight, 0.21 to 0.40 was fair, 0.41 to 0.60 was moderate, 0.61 to 0.80 was substantial, and 0.8 to 1 was good to very good. ROC analysis with determination of the AUC and a corresponding 95% confidence interval (95% CI) was performed to evaluate ADCmean and ADCmin diagnostic

values for lymph node characterization. $P < 0.05$ was considered statistically significant.

RESULTS

Patients' Characteristics

Twenty-four patients with untreated LARC were included in the statistical analysis (18 men, 6 women; mean age, 64 ± 12 years [range, 45–87 years]). Twenty patients (83%) had a T3 stage tumor, and 4 patients (17%) had a T4 stage tumor, which were all histologically characterized as rectal adenocarcinoma. Of the 24 tumors, 4 were located in the lower third, 13 in the middle third, and 7 in the upper third of the rectum. The mean distance from the tumor to the anal verge was 67 ± 27 mm, and the mean longitudinal extension was 54 ± 25 mm. Twenty-two tumors displayed spicules in the mesorectal fat, among which 10 along the anterior wall, 6 along the posterior wall, and 10 along the lateral walls of the rectum.

Rectal Cancer Results

SUVmax and SUVmean values of the rectal cancers ($n = 24$) were 17.5 ± 8.2 and 13.3 ± 6.1 g/mL, respectively, whereas their ADCmin and ADCmean values were $787 \pm 185 \times 10^{-6} \text{ mm}^2/\text{s}$ and $1057 \pm 218 \times 10^{-6} \text{ mm}^2/\text{s}$, respectively. There was no statistically significant difference of SUVmax, SUVmean, ADCmin, or

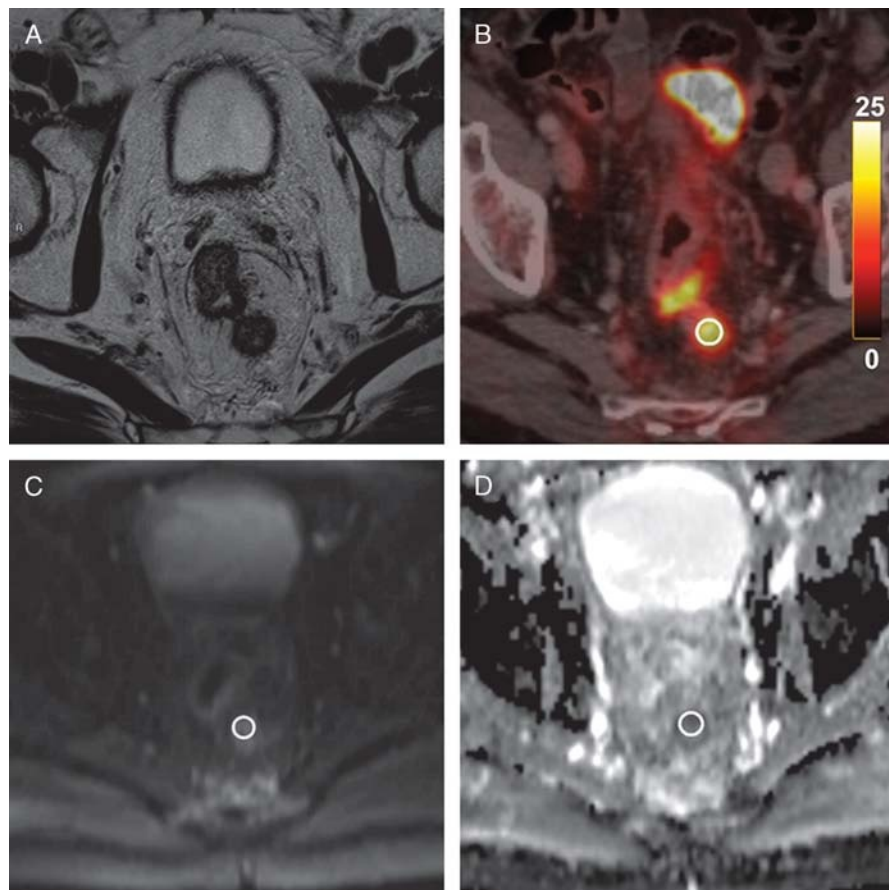


FIGURE 2. Pathological lymph node in a 69-year-old man with a T4 N2 stage rectal cancer. **A**, Axial T2-weighted MR image shows a pathological lymph node located in the posterior mesorectum. **B**, Axial ^{18}F -FDG PET/CT demonstrates high ^{18}F -FDG uptake of this same lymph node (SUVmean = 8.9 g/mL, SUVmax = 10.7 g/mL). **C** and **D**, Axial diffusion-weighted image and ADC map show a focal diffusion restriction within the lymph node (ADCmean = $1047 \times 10^{-6} \text{ mm}^2/\text{s}$, ADCmin = $763 \times 10^{-6} \text{ mm}^2/\text{s}$).

ADCmean between T3 and T4 tumors ($P > 0.19$). The difference of SUVmax, SUVmean, ADCmin, or ADCmean was not statistically significant for tumors in different rectal locations or the presence of spicules ($P > 0.14$, Table 2).

As for the rectal cancer, we found a substantial significant negative correlation between the SUVmean and the corresponding ADCmean values ($\rho = -0.61$, $P = 0.0017$) (Fig. 3) and between

ADCmin and SUVmax values ($\rho = -0.66$, $P = 0.0005$). SUVmax, SUVmean, ADCmin, and ADCmean were not significantly correlated with longitudinal tumor extension ($P > 0.08$).

Regional Lymph Node Results

In total, 44 pathological and 19 control lymph nodes were evaluated. Among the 44 pathological regional lymph nodes we

TABLE 2. Rectal Tumors SUV and ADC Values

Tumors	n	SUVmean, g/mL	P	SUVmax, g/mL	P	ADCmean, $\times 10^{-6} \text{ mm}^2/\text{s}$	P	ADCmin	P
All	24	13.3 \pm 6.1		17.5 \pm 8.2		1057 \pm 218		787 \pm 185	
Stage									
T3	20	12.5 \pm 5.7	0.22	16.3 \pm 7.5	0.19	1080 \pm 228	0.28	799 \pm 200	0.64
T4	4	17.6 \pm 6.7		23.6 \pm 10.2		942 \pm 115		726 \pm 53	
Location									
Low rectum	4	15.6 \pm 9.1	0.8	22.6 \pm 12.6	0.8	1108 \pm 250	0.92	898 \pm 300	0.36
Mid rectum	13	13.1 \pm 6.0		17.2 \pm 8.0		1058 \pm 242		744 \pm 183	
High rectum	7	12.4 \pm 4.9		15.1 \pm 5.4		1024 \pm 175		804 \pm 83	
Spicules									
Present	22	13.5 \pm 6.3	0.83	17.7 \pm 8.6	1.0	1070 \pm 223	0.14	792 \pm 187	0.83
Absent	2	11.3 \pm 1.1		15.3 \pm 0.8		914 \pm 56		733 \pm 211	

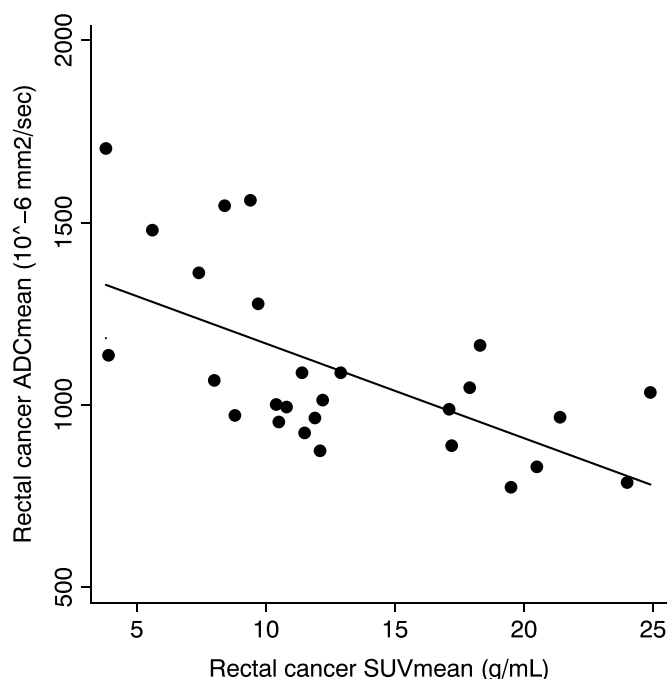


FIGURE 3. Correlation ($\rho = -0.61$, $P = 0.0017$) between ADCmean and SUVmean of the rectal tumor before treatment.

had assessed, there were 33 perirectal, 6 internal iliac, 3 external iliac, 1 common iliac, and 1 inguinal lymph nodes. The size of pathological and control lymph nodes was not significantly different (8.3 ± 3.7 vs 7.2 ± 1.4 mm, $P = 0.41$). The mean SUVmax and SUVmean were significantly higher in the pathological lymph nodes than in the control lymph nodes (7.0 ± 5.4 vs 1.3 ± 0.5 g/mL and 5.0 ± 3.7 vs 1.0 ± 0.4 g/mL, $P = 0.0001$). This was the case for pathological lymph nodes equal to or smaller than 1 cm ($n = 38$, $P = 0.0003$) or larger than 1 cm ($n = 6$, $P = 0.0001$). ADCmean was significantly lower in pathological lymph nodes (1099 ± 185 vs $1379 \pm 324 \times 10^{-6}$ mm²/s, $P = 0.0012$) than in control lymph nodes. This was the case for pathological lymph nodes equal to or smaller than 1 cm ($n = 38$, $P = 0.003$) or larger than 1 cm ($n = 6$, $P = 0.009$). ADCmin was not significantly different between pathological and control lymph nodes (821 ± 214 vs $890 \pm 400 \times 10^{-6}$ mm²/s, $P = 0.27$). This was the case for pathological lymph nodes equal to or smaller than 1 cm ($n = 38$, $P = 0.38$) or larger than 1 cm ($n = 6$, $P = 0.16$).

Taking into account all pathological and control lymph nodes ($n = 63$), ADCmean showed a fair but statistically significant negative correlation with the corresponding SUVmean values ($\rho = -0.38$, $P = 0.0021$). There was, however, no statistically significant correlation between ADCmin and SUVmax ($\rho = -0.11$, $P = 0.41$). SUVmean and SUVmax values were statistically significantly correlated with lymph node size ($\rho = 0.42$, $P < 0.0007$), but there was no statistically significant correlation between lymph node size and ADC mean ($\rho = -0.08$, $P = 0.54$) or ADCmin ($\rho = -0.06$, $P = 0.62$) values.

With AUCs of 0.24 (95% CI, 0.10–0.38) and 0.41 (95% CI, 0.22–0.60), respectively, neither ADCmean nor ADCmin values allowed for accurate distinction between pathological and control lymph nodes when compared with the combination of morphological MRI and PET/CT criteria.

DISCUSSION

PET/CT and DW-MRI are 2 complementary modalities used for initial staging in primary rectal cancer, providing information about metabolic activity and cellularity. Both modalities provide information about tumor features and have been shown to be useful in evaluating tumor response to treatment.^{14–17}

The purposes of this study were to assess the relation between quantitative parameters resulting from DW-MRI and ¹⁸F-FDG PET/CT imaging of regional lymph nodes in untreated LARC and the associated primary tumor, as well as to determine the diagnostic performance of ADC values in identifying pathological lymph nodes. We found a statistically significant correlation between ADCmean and SUVmean for the regional lymph nodes and the rectal tumor. To the best of our knowledge, our study is the first that confirms an association between the tumor cellularity and the metabolic activity both in pathological lymph nodes and the related untreated LARC.^{11,12} ADCmin and ADCmean did not, however, help differentiate pathological from benign lymph nodes.

In rectal cancer, the correct initial local staging is important for distinguishing between locally advanced tumors (T3 and T4) and less invasive tumors (T1 and T2) when choosing the optimal treatment (surgery, neoadjuvant chemoradiotherapy, radiotherapy, or chemotherapy alone). As the neoplastic specimen (primary tumor or lymph node) is not available for histological examination prior to treatment, imaging is of paramount importance. Endorectal US, CT, and MRI have been widely used for rectal cancer staging.¹⁸ As to MRI, field strengths of either 3 T or 1.5 T may be used.¹⁹ Indeed, a direct comparison²⁰ could not reveal any improved accuracy in T staging of rectal cancer when using 3-T MR scanners despite their 2-fold increase in the signal-to-noise ratio compared with 1.5-T MR machines.

Because most primary rectal tumors show intense ¹⁸F-FDG uptake,⁶ ¹⁸F-FDG PET/CT has also emerged as a promising option for the staging of LARC. It can correctly identify 94.6% of rectal adenocarcinomas and define their local extension (T stage) with an accuracy of 94.3% (95% CI, 87%–100%).²¹ Only a few studies have reported a comparison between the SUV uptake of ¹⁸F-FDG PET/CT and the ADC values generated from DWI for the initial quantitative assessment of primary rectal tumors. In our study, we did not find any statistically significant difference of tumor SUVmax, SUVmean, ADCmin, or ADCmean for tumors with different T stages or locations within the rectum. Curvo-Semedo et al⁸ showed that lower ADCmean values are associated with a more aggressive tumor profile and are significantly correlated with the mesorectal fascia extension seen on MRI and with their grade of differentiation. To the contrary, we found neither any statistically significant difference of tumor SUV or ADC with respect to the presence or absence of perirectal spicules, nor any relation between SUV or ADC and longitudinal tumor extension. This suggests, as previously reported by Uchiyama et al,²² that the primary tumor morphology may not necessarily be related to metabolism or cellularity. However, we found a statistically significant negative correlation between ADCmean and the corresponding SUVmean values ($\rho = -0.61$, $P = 0.0017$) and between ADCmin and SUVmax ($\rho = -0.66$, $P = 0.0005$) values. Two previous studies^{11,12} have shown a significant negative correlation between ADCmin and SUVmax ($r = -0.450$, $P = 0.009$; and $r = -0.347$, $P = 0.026$, respectively) for primary rectal adenocarcinoma. In these studies, ADCmin was determined as the lowest value and SUVmax as the highest value among all voxels of the entire volume in each tumor. However, there was no certitude that the tumor area with the maximum SUV value corresponded to the tumor area with the minimum ADC value.^{11,12} Unlike these authors, we spatially coregistered our DWI with ¹⁸F-FDG PET/CT images after drawing a 1-cm² ROI

around the rectal tumor area with the highest ^{18}F -FDG uptake to determine SUVmax. Thus, we aimed at obtaining a perfect anatomic correlation for the 2 imaging modalities in order to be able to compare SUVmax and ADCmin values as true comparables. With the same rigid anatomic coregistration, we similarly assessed the relation between SUVmean and ADCmean values, which may explain the stronger correlation ($\rho = -0.61$, $P = 0.0017$) compared with the values reported by Gu et al¹¹ ($r = -0.402$, $P = 0.02$).

The exact staging of regional lymph node status is also mandatory for determining the optimal therapy. Size, shape, delineation, and texture of lymph nodes are morphological criteria used for characterization, but none has proven to be a sufficient criterion.⁵ In concordance with Monig et al, who found that size is not a good criterion for differentiating metastatic from disease-free lymph nodes,²³ we did not find any statistically significant difference in size between pathological and control lymph nodes. For the detection of malignant lymph nodes, PET/CT has a sensitivity of 61%, with a high specificity of 83%, whereas MRI has a high sensitivity of 94%, but a specificity of only 67%.¹³ Combining high-resolution pelvic MRI and ^{18}F -FDG PET/CT improves the accuracy of nodal status prediction.¹³ Diffusion-weighted imaging can also facilitate lymph node detection better than T2-weighted MR sequences can, but without being reliable for differentiating between benign and malignant lymph nodes (AUC = 0.45–0.64).^{24,25} Evaluating 196 histologically benign and 16 histologically malignant lymph nodes, Heijnen et al²⁴ also reported that the ADCmean value was higher for benign lymph nodes (1.150 ± 0.24 vs $1.04 \pm 0.22 \times 10^{-3}$ mm²/s), although not statistically significant ($P = 0.10$), probably because of insufficient reproducibility of ADC measurement in the lymph nodes.²⁶ We hereby confirm and extend these results by demonstrating that the ADCmean, but not the ADCmin value, was lower in pathological regional lymph nodes, regardless of pathological lymph node size. With an AUC of less than 0.50 on ROC analysis, ADC values were, however, not reliable for accurately distinguishing between pathological and benign lymph nodes at initial staging. To the best of our knowledge, only Cho et al²⁷ reported that ADC values help identify metastatic lymph nodes using radiological-pathological correlation of all lymph nodes greater than 2 mm in surgical specimens in patients with rectal cancer. Some concerns regarding the methodology may explain the nonreproducibility of these results. First, the difference in size between benign and malignant nodes (3.5 ± 1.6 vs 6.4 ± 3.3 mm, $P < 0.0001$) could have influenced the ADC values because of background noise, although interobserver agreement was good. Second, the exact spatial correlation of lymph nodes with a diameter of less than 5 mm between DWI and macroscopic surgical specimens may be questionable regarding tissues shrinking after resection, as indirectly confirmed by the high exclusion rate of lymph nodes in this study ($354/468 = 76\%$). While ADC values did not identify pathological lymph nodes, a significant negative correlation between SUVmean and ADCmean of the lymph nodes was found, suggesting an association between metabolism and cellularity of the primary rectal tumor, similarly to other cancers.^{9,28}

Hybrid FDG PET/MRI has been reported as an evolving tool for the workup of advanced rectal cancer,^{29,30} thus combining the excellent soft tissue contrast of MRI and the high sensitivity for N and M staging inherent in PET. Preliminary results suggest that PET/MRI allows for more detailed T staging than PET/CT,²⁹ but the accuracy in N staging does not seem to change significantly, when compared with PET/CT.^{29,30}

We have to address some limitations of our study. First, no histopathologic analysis of our included lymph nodes was available. Because we included only LARC, all our patients immediately underwent neoadjuvant radiochemotherapy after initial staging and

before surgery. Because of morphological changes induced by the neoadjuvant therapy, histological analysis could not be used as the standard of reference in these settings. However, using automatic coregistration software, we obtained perfect anatomic correlation for measuring ^{18}F -FDG PET/CT and DWI quantitative parameters in both tumors and lymph nodes when compared with previously published studies using these methods. Second, ^{18}F -FDG PET/CT examination was performed on a Discovery 690 PET/CT scanner (GE Healthcare, Milwaukee, Wis). Owing to a transverse spatial resolution (4.7 mm) higher than that of PET scanners used in previous studies (6.7–9 mm),^{12,21} SUVmax and SUVmean values may be significantly increased for small lesions such as lymph nodes because of partial volume effect reduction, thus limiting the possibility of comparing the studies.

In conclusion, we report a statistically significant negative correlation between ADCmean and SUVmean values both in primary LARC and regional lymph nodes in the same patient population, thus confirming an association between tumor cellularity and metabolic activity. ADC values were, however, unreliable for purposes of distinguishing between pathological and normal lymph nodes.

ACKNOWLEDGEMENTS

The authors thank the team of technologists of the Department of Radiodiagnostic and Interventional Radiology and Nuclear Medicine and Molecular Imaging for performing the MR and PET/CT examinations.

REFERENCES

1. Ferlay J, Steliarova-Foucher E, Lortet-Tieulent J, et al. Cancer incidence and mortality patterns in Europe: estimates for 40 countries in 2012. *Eur J Cancer*. 2013;49:1374–1403.
2. Garland ML, Vather R, Bunkley N, et al. Clinical tumour size and nodal status predict pathologic complete response following neoadjuvant chemoradiotherapy for rectal cancer. *Int J Colorectal Dis*. 2014;29:301–307.
3. Kim SH, Lee JM, Park HS, et al. Accuracy of MRI for predicting the circumferential resection margin, mesorectal fascia invasion, and tumor response to neoadjuvant chemoradiotherapy for locally advanced rectal cancer. *J Magn Reson Imaging*. 2009;29:1093–1101.
4. Beets-Tan RG, Beets GL, Vliegen RF, et al. Accuracy of magnetic resonance imaging in prediction of tumour-free resection margin in rectal cancer surgery. *Lancet*. 2001;357:497–504.
5. Beets-Tan RG, Lambregts DM, Maas M, et al. Magnetic resonance imaging for the clinical management of rectal cancer patients: recommendations from the 2012 European Society of Gastrointestinal and Abdominal Radiology (ESGAR) consensus meeting. *Eur Radiol*. 2013;23:2522–2531.
6. Llamas-Elvira JM, Rodriguez-Fernandez A, Gutierrez-Sainz J, et al. Fluorine-18 fluorodeoxyglucose PET in the preoperative staging of colorectal cancer. *Eur J Nucl Med Mol Imaging*. 2007;34:859–867.
7. Burt BM, Humm JL, Kooby DA, et al. Using positron emission tomography with [(18)F]FDG to predict tumor behavior in experimental colorectal cancer. *Neoplasia*. 2001;3:189–195.
8. Curvo-Semedo L, Lambregts DM, Maas M, et al. Diffusion-weighted MRI in rectal cancer: apparent diffusion coefficient as a potential noninvasive marker of tumor aggressiveness. *J Magn Reson Imaging*. 2012;35:1365–1371.
9. Schmidt S, Dunet V, Koehli M, et al. Diffusion-weighted magnetic resonance imaging in metastatic gastrointestinal stromal tumor (GIST): a pilot study on the assessment of treatment response in comparison with ^{18}F -FDG PET/CT. *Acta Radiol*. 2013;54:837–842.
10. Regier M, Derlin T, Schwarz D, et al. Diffusion weighted MRI and ^{18}F -FDG PET/CT in non-small cell lung cancer (NSCLC): does the apparent diffusion coefficient (ADC) correlate with tracer uptake (SUV). *Eur J Radiol*. 2012;81:2913–2918.
11. Gu J, Khong PL, Wang S, et al. Quantitative assessment of diffusion-weighted MR imaging in patients with primary rectal cancer: correlation with FDG-PET/CT. *Mol Imaging Biol*. 2011;13:1020–1028.

12. Colakoglu Er H, Erden A, Kucuk NO, et al. Correlation of minimum apparent diffusion coefficient with maximum standardized uptake on fluorodeoxyglucose PET-CT in patients with rectal adenocarcinoma. *Diagn Interv Radiol*. 2013;20:105–109.
13. Kim DJ, Kim JH, Ryu YH, et al. Nodal staging of rectal cancer: high-resolution pelvic MRI versus ¹⁸F-FDGPET/CT. *J Comput Assist Tomogr*. 2011;35:531–534.
14. Capirci C, Rampin L, Erba PA, et al. Sequential FDG-PET/CT reliably predicts response of locally advanced rectal cancer to neo-adjuvant chemo-radiation therapy. *Eur J Nucl Med Mol Imaging*. 2007;34:1583–1593.
15. Calvo FA, Domper M, Matute R, et al. ¹⁸F-FDG positron emission tomography staging and restaging in rectal cancer treated with preoperative chemoradiation. *Int J Radiat Oncol Biol Phys*. 2004;58:528–535.
16. Lambrecht M, Deroose C, Roels S, et al. The use of FDG-PET/CT and diffusion-weighted magnetic resonance imaging for response prediction before, during and after preoperative chemoradiotherapy for rectal cancer. *Acta Oncol*. 2010;49:956–963.
17. Ippolito D, Monguzzi L, Guerra L, et al. Response to neoadjuvant therapy in locally advanced rectal cancer: assessment with diffusion-weighted MR imaging and ¹⁸F-FDG PET/CT. *Abdom Imaging*. 2012;37:1032–1040.
18. Bipat S, Glas AS, Slors FJ, et al. Rectal cancer: local staging and assessment of lymph node involvement with endoluminal US, CT, and MR imaging—a meta-analysis. *Radiology*. 2004;232:773–783.
19. Kim CK, Kim SH, Chun HK, et al. Preoperative staging of rectal cancer: accuracy of 3-Tesla magnetic resonance imaging. *Eur Radiol*. 2006;16:972–980.
20. Maas M, Lambregts DMJ, Lahaya MJ, et al. T-staging of rectal cancer: accuracy of 3 T compared with 1.5 T. *Abdom Imaging*. 2012;37:475–481.
21. Mainenti PP, Iodice D, Segreto S, et al. Colorectal cancer and ¹⁸F-FDG-PET/CT: what about adding the T to the N parameter in loco-regional staging? *World J Gastroenterol*. 2011;17:1427–1433.
22. Uchiyama S, Haruyama Y, Asada T, et al. Role of the standardized uptake value of 18-fluorodeoxyglucose positron emission tomography-computed tomography in detecting the primary tumor and lymph node metastasis in colorectal cancers. *Surg Today*. 2012;42:956–961.
23. Monig SP, Schroder W, Baldus SE, et al. Preoperative lymph-node staging in gastrointestinal cancer—correlation between size and tumor stage. *Onkologie*. 2002;25:342–344.
24. Heijnen LA, Lambregts DM, Mondal D, et al. Diffusion-weighted MR imaging in primary rectal cancer staging demonstrates but does not characterise lymph nodes. *Eur Radiol*. 2013;23:3354–3360.
25. Lambregts DM, Maas M, Riedl RG, et al. Value of ADC measurements for nodal staging after chemoradiation in locally advanced rectal cancer—a per lesion validation study. *Eur Radiol*. 2011;21:265–273.
26. Kwee TC, Takahara T, Luijten PR, et al. ADC measurements of lymph nodes: inter- and intra-observer reproducibility study and an overview of the literature. *Eur J Radiol*. 2010;75:215–220.
27. Cho EY, Kim SH, Yoon JH, et al. Apparent diffusion coefficient for discriminating metastatic from non-metastatic lymph nodes in primary rectal cancer. *Eur J Radiol*. 2013;82:e662–e668.
28. Ho KC, Lin G, Wang JJ. Correlation of apparent diffusion coefficients measured by 3T diffusion-weighted MRI and SUV from FDG PET/CT in primary cervical cancer. *Eur J Nucl Med Mol Imaging*. 2009;36:200–208.
29. Paspulati RM, Partovi S, Herrmann KA, et al. Comparison of hybrid FDG PET/MRI compared with PET/CT in colorectal cancer staging and restaging: a pilot study. *Abdom Imaging*. 2015;40:1415–1425.
30. Buchbender C, Heusner TA, Lauenstein TC, et al. Oncologic PET/MRI, part 1: tumors of the brain, head and neck, chest, abdomen, and pelvis. *J Nucl Med*. 2012;53:928–938.